

Towards 3D inversion of ground based TEM data

Kristoffer R Andersen*

Aarhus University
C.F. Møllers Alle 4
8000 Aarhus C
Denmark
kristoffer@geo.au.dk

Casper Kirkegaard

Aarhus University
C.F. Møllers Alle 4
8000 Aarhus C
Denmark
casperk@geo.au.dk

Esben Auken

Aarhus University
C.F. Møllers Alle 4
8000 Aarhus C
Denmark
esben.auken@geo.au.dk

Anders V Christiansen

Aarhus University
C.F. Møllers Alle 4
8000 Aarhus C
Denmark
anders.vest@geo.au.dk

SUMMARY

We describe the setup for inversion of ground based TEM data using a 3D modelling code and a full description of the measurement system using the system response. The response is calculated using a finite volume method where we solve for the electric field on the edges of a staggered grid and time step solutions using backward Euler steps. For the forward calculation we use an iterative solver and a preconditioner which solves the Helmholtz decomposed E-fields. In the iterative process we take advantage of the similarity between different time steps and always use the previous result as the starting point of the next iteration. To compare the calculated fields with measured data we interpolate the fields to the receiver positions and convolute the calculated fields with the system response. In this way we include all system related effects in the calculation and this is in particular relevant for the early time signal. We show that the forward code is in good agreement with the analytic response from a half space and sketch the layout of survey setup with a large, centrally positioned transmitter and many receivers located around the transmitter. We demonstrate that the code can be used to invert data from a single loop system with multiple receivers as commonly used in ground follow-up surveys in mineral exploration.

Key words: 3D TEM, inversion, system modelling.

INTRODUCTION

1D TEM inversions have been used for years and these inversions are generally reliable, fast and accurate. There are several inversion frameworks for such inversions which incorporate different kinds of constraints. These constraints are in the simplest case only constraining the 1D conductivity model, but in more advanced frameworks the 1D inversions are also constrained along the line of soundings (often referred to as laterally constrained inversions, LCI) or even inter-line constraints like the spatially constrained inversions (SCI) (Viezzoli, et al. 2008). Such inversions generate conductivity models where the model description is quasi-3D or full 3D, but the forward modelling is only performed in 1D. This is in many cases accurate, especially if the geology is mainly sedimentary and the topology is flat. However, there are cases where the 1D inversion leads to inaccurate results. This happens e.g. where sharp vertical conductivity contrasts are present, and we see the so-called pant legs in the 1D inversions (Newman, et al. 1987). Furthermore, the 1D codes are becoming increasingly fast, and therefore even very large surveys can be inverted within fairly short time (Kirkegaard, et al. 2015).

The natural successor to the 1D inversions are full 3D inversions, where the full model is used for forward calculations, and topography can naturally be included in the calculation. 3D inversion frameworks have only recently become available and only a few groups in the world have 3D codes for TEM calculations. These calculations are generally computationally heavy and need finely optimized codes that benefit from modern hardware architecture and large clusters. The codes are generally either finite volume codes (Oldenburg, et al. (2013), Haber and Schwarzbach (2014), Haber (2015)), finite element codes (Borner, et al. 2008) or integral equation codes (Cox, et al. 2010).

We have written a finite volume code using staggered grids (Kane 1966) and use an iterative solver for the forward and the inversion problem. We invert single transmitter, ground based TEM soundings, and describe the full system setup using the so-called system response, which includes a full description of the transmitter waveform and the receiver system. This code is the first step towards a full inversion framework for airborne TEM surveys, where a full survey is split into subdomains, and 3D TEM forward calculations are performed on the individual domains. In the inversion, the full survey is handled collectively and thereby includes regularizations across the domains. Here we briefly describe the theoretical basis of the forward problem and include the system description. We show the survey layout for a ground based TEM survey, and compare the 3D forward response to the analytic solution for a half space.

METHOD AND RESULTS

We initially set up the relevant equations describing the 3D problem and explain the grids used for the calculations. Starting from Maxwell's equations and using the quasi-static approximation ($\epsilon = 0$) we have

$$\nabla \times E = -\mu \frac{dH}{dt},$$

$$\nabla \times H = \sigma E + s,$$

where s is some source term. We discretise the temporal derivative using a backward Euler discretization and solve for the electric field

$$\nabla \times \frac{1}{\mu} \nabla \times E^i + \frac{1}{\Delta t} \sigma E^i = \frac{1}{\Delta t} \sigma E^{i-1},$$

where the source term is set to zero. We calculate the initial steady state field and use that as the initial condition for the differential equation. Spatially we discretise the system on a regular grid given by three vectors \vec{x} , \vec{y} , and \vec{z} . We use a staggered grid where the electric fields are positioned on the cell edges and the magnetic fields are positioned on the cell faces as shown in Figure 1. To every cell we assign a conductivity σ and for cells in the air we lock the conductivity to 10^{-7} S/m. Since the perpendicular component of the electric field is discontinuous across an interface, we avoid having perpendicular components of the electric field at interfaces by putting the electric fields on the edges. Furthermore, by displacing the magnetic fields from the electric fields as done in the staggered grid we naturally obtain the spatial derivatives at the right positions. The grid is shown in Figure 1.

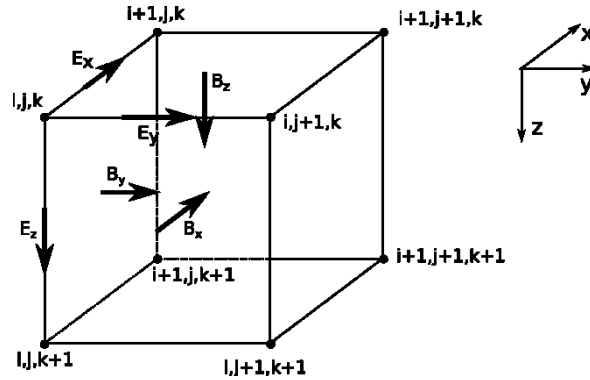


Figure 1: The staggered grid with the electric fields on the edges and the magnetic fields perpendicular to the faces. This positioning of the fields naturally fits the spatial derivatives used in Maxwell's equations.

The solution for the electric field can now be time-stepped forward from some initial field. We calculate the initial field from an initial steady-state current consisting of N pieces of straight wire. However, one could also use other initial fields such as the field from a circular source. We prefer the generality of the present case, which can also approximate a circular current source very well. The vector potential at position $r = (x,y,z)$ from a line current from $r_1=(0,0,0)$ to $r_2=(l,0,0)$ is given by the analytic expression

$$A = \frac{1}{4\pi} \begin{pmatrix} \log(\sqrt{x^2 + y^2 + z^2 + x}) - \log(\sqrt{(x-l)^2 + y^2 + z^2 + (x-l)}) \\ 0 \\ 0 \end{pmatrix},$$

and the magnetic field can be found by applying the curl operation. In this way we also ensure that the magnetic field is divergence free. Once the magnetic field is known we can find the electric field from $\nabla \times H = \sigma E$ (for steady state and no sources s).

Once the electric field is calculated we find dB/dt , which is measured by the receivers in the TEM survey. This is easily obtained using Faraday's law. Since the field is only known at specific locations on the grid, one has to interpolate to a general position. The simplest case is to use a linear interpolation, but more advanced interpolations can also be used. With the time evolution of the magnetic induction at the receiver position, we can compare the measured signal to the calculated. Since the measured signal is influenced by several other factors such as; the transmitter waveform, receiver coil characteristics, and receiver electronics. One has to take these into account. The waveform can naturally be incorporated into the forward calculation by including a time evolution of the source term. Alternatively, one can calculate the field from a step turn-off current and subsequently convolute the calculated field with the waveform. The receiver cannot directly be put into the forward modelling and has to be handled afterwards. We chose to combine all the effects into a single system response, which is convoluted with the calculated field (Andersen, et al. 2015). The system response is given by

$$SR = \frac{1}{I_{max}} \frac{dI}{dt} * h_{coil} * h_{amplifier}$$

where I_{max} is the peak transmitter current, I is the transmitter waveform, h_{coil} is the impulse response of the receiver coil and $h_{amplifier}$ is the impulse response of the amplifier. The measured signal is given by

$$signal(t,r) = \int SR(s) \cdot FWR(t-s,r) ds$$

where FWR both contains an interpolation to the receiver position r and a temporal interpolation to time $t-s$. For the simplest case where both interpolations are linear these operations can be written as matrices. In other words one can write

$$FWR(t, r) = P_{time}(t)P_{space}(r)u,$$

where u is the solution vector to the forward problem and P_{time} and P_{space} are two interpolation matrices.

The system response is plotted in Figure 2. It is mainly relevant to take into account the system response for the early gates, where the time dependence of the waveform and the receiver plays the largest role. With a 300 kHz 1st order Butterworth filter, the signal is effectively broadened by some μ s. This does not play a large role for the late gates that mainly probe the deepest parts of the model, but it has a large effect on the early gates where the near-surface is probed. With the time-stepping solution used to solve Maxwell's equation we automatically obtain the signal at early times necessary for the convolution with the system response.

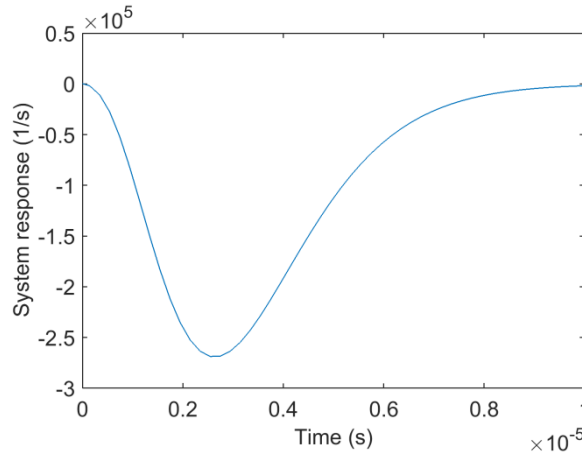


Figure 2: System response for the ramp-down of the TEM system. The system response includes the time derivative of the transmitter waveform and the receiver system.

We invert data from a ground based, single transmitter and multiple receiver setup. A sketch of the setup is shown in Figure 3 where the large square transmitter and many small receivers are positioned in the central, regular part of the grid. Outside the regular grid a padding grid is used, where the cell sizes are exponentially increasing. The figure is not to scale and only shows a sketch of the setup.

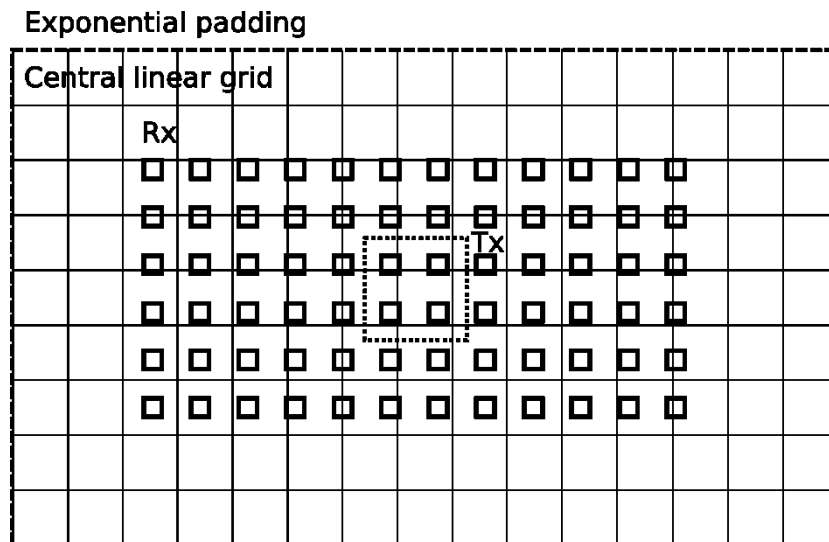


Figure 3: Sketch (not to scale) of the measurement setup with a large transmitter loop in the center and many small receivers around the transmitter. The central part of the calculation grid is linearly spaced and the outer padding has exponentially increasing grid cells. The padding grid is not shown.

The forward problem is solved using an iterative solver. However, due to the large null space of the curl operator one has to carefully choose the preconditioner. Presently we use the Helmholtz decomposition $E = A + \nabla\Phi$ to eliminate this null-space and approximately solve the (A, Φ) -system using one iteration of Gauss-Seidel. When solving this we benefit significantly from using the previous result as the starting point for the next iteration. We are also planning on implementing a preconditioner using an incomplete-LU factorization and consider using algebraic multigrid. With the present setup we can solve one time step of a 51^3 grid in ~10-15 seconds on 1 CPU, and we know from experience that our iterative solvers generally scale very well when using more CPUs. For the first time steps the solver needs more iterations compared to the later steps, and therefore the time needed to calculate a time step changes during the forward calculation.

Since the setup only uses one transmitter, the equations only have to be solved once and the result is interpolated to all the receiver positions. For the conductivity model we use a different grid and map the conductivity onto the forward cells. The derivatives with respect to the model mesh are obtained using the chain rule. Regularizations are used in the model along both the horizontal- and vertical direction. For the inversion we use the adjoint state method (Plessix 2006) to calculate the derivatives of the optimisation function with respect to the model parameters and the BFGS method to estimate the 2nd derivative from the 1st derivatives.

A forward calculation for an approximately circular transmitter loop (10 straight wires) on the ground of a 10 Ωm half space is shown in Figure 4 for a receiver in the center of the transmitter. Here a 50^3 grid was used with the smallest cell size being $(2.5\text{m})^3$. The response is compared to the analytic response and a good agreement is observed. For the conference we will show inversions using the setup described and an iterative solver.

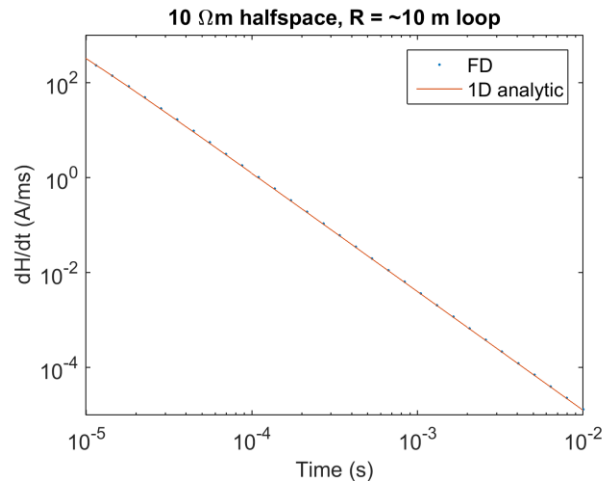


Figure 4: The forward response for a 10 wire piece loop source (approx. 10 m radius) on the ground of a 10 Ωm half space and compared to the analytic 1D response.

CONCLUSIONS

We describe the setup for 3D inversions of ground based TEM data where the full system description is taken into account in the forward modelling. We solve for the electric field on a staggered grid, calculate dB/dt by taking the curl of the E field, and convolute the magnetic field with the system response which includes all system related effects and therefore can accurately model the very early time response which probes the near-surface. For the inversion the adjoint state method is used together with the BFGS method.

ACKNOWLEDGMENTS

We acknowledge support from the Danish Innovation Fund, which funded the project AirTech4Water under which the present research was performed.

REFERENCES

- Andersen, K.R., Nyboe, N.S., Kirkegaard, C., Auken, E., and Christiansen, A.V., 2015. A System Response Convolution Routine for Improved near Surface Sensitivity in Skytem Data. *EAGE First European Airborne Electromagnetics Conference*, Tu AEM 07.
- Borner, R.U., Ernst, O.G., and Spitzer, K., 2008, Fast 3-D Simulation of Transient Electromagnetic Fields by Model Reduction in the Frequency Domain Using Krylov Subspace Projection. *Geophysical Journal International* **173**, 766-80.
- Cox, L.H., Wilson, G.A., and Zhdanov, M.S., 2010, 3d Inversion of Airborne Electromagnetic Data Using a Moving Footprint. *Exploration Geophysics* **41**, 250-59.
- Haber, E., 2015, *Computational Methods in Geophysical Electromagnetics*. Society of Industrial and Applied Mathematics.
- Haber, E. and Schwarzbach, C., 2014, Parallel Inversion of Large-Scale Airborne Time-Domain Electromagnetic Data with Multiple Octree Meshes. *Inverse Problems*, 1-29.
- Kane, Y., 1966, Numerical Solution of Initial Boundary Value Problems Involving Maxwell's Equations in Isotropic Media. *Antennas and Propagation, IEEE Transactions on* **14**, 302-07.
- Kirkegaard, C., Andersen, K., Boesen, T., Christiansen, V., Auken, E., and Fiandaca, G., 2015, Utilizing Massively Parallel Co-Processors in the Aarhusinv 1d Forward and Inverse Aem Modelling Code. *ASEG Extended Abstracts 2015*, 1-3.

Newman, G.A., Anderson, W.L., and Hohmann, G.W., 1987, Interpretation of Transient Electromagnetic Soundings over Three-Dimensional Structures for the Central-Loop Configuration. *Geophysical Journal Of The Royal Astronomical Society* **89**, 889-914.

Oldenburg, D.W., Haber, E., and Shekhtman, R., 2013, Three Dimensional Inversion of Multisource Time Domain Electromagnetic Data. *Geophysics* **78**, E47-E57.

Plessix, R.E., 2006, A Review of the Adjoint-State Method for Computing the Gradient of a Functional with Geophysical Applications. *Geophysical Journal International* **167**, 495-503.

Viezzoli, A., Christiansen, A.V., Auken, E., and Sørensen, K.I., 2008, Quasi-3d Modeling of Airborne Tem Data by Spatially Constrained Inversion. *Geophysics* **73**, F105-F113.